Dynamical branching during fluorination of the dimerized Si(100) surface: A molecular dynamics study

Thomas A. Weber
Division of Advanced Scientific Computing, National Science Foundation, Washington, D. C. 20550

Frank H. Stillinger
AT&T Bell Laboratories, Murray Hill, New Jersey 07974

(Received 23 October 1989; accepted 2 February 1990)

Collections of classical trajectories have been numerically generated for individual F_2 molecules impinging at normal incidence on a Si(100) surface at 0 K dimerized in a $p(2\times1)$ pattern. A linear combination of two-atom and three-atom interaction functions represents the potential energy. Trajectories fall into four categories: (a) nonreactive F_2 rebound, (b) monofluorination at a surface dangling bond with energetic expulsion into the vacuum of the remaining F atom, (c) difluorination of a pair of dangling bonds, and (d) monofluorination with retention of the second F in a weakly bound Si–F···F surface complex. Surface patterns for difluorination, (c), indicate absence of surface diffusion during this mode of chemisorption. Increasing either the translational kinetic energy or the vibrational excitation of the incident F_2 appears to enhance its surface reactivity.

I. INTRODUCTION

Surface science offers a wide range of fascinating phenomena, among the most significant of which are those involving chemical reactions.[1] Many experimental techniques are available to study surface reactions, but since the processes involved are usually very complex at the atomic level, any new method to supplement those already available should indeed be welcome. Our main objective is to demonstrate the utility of computer simulation as a potentially valuable adjunct to experiment, specifically in cases of chemical reaction between a solid substrate and an ambient gas.

We confine attention herein to fluorination of the dimerized (100) surface of crystalline silicon, a case with some technological relevance.[2] Except for a minor technical modification explained below, the model employed is the same one that we used recently to simulate rapid exothermic etching of silicon by high density fluorine gas.[3] However, now the emphasis is on extraction of dynamical details in the simpler circumstance that single F_2 molecules impinge on an unreacted (but dimerized) silicon surface. Several outcomes are possible at each surface collision, with branching ratios that depend on initial conditions. The molecular dynamics simulations reported below were designed to determine such dependence, at least in part.

Section II specifies the potential energy function employed. Section III explains boundary and initial conditions used for our dynamical simulations, and provides algorithmic details. Our results are presented in Sec. IV. The paper concludes with a final Sec. V containing discussion and conclusions.

II. MODEL

The surface phenomena under consideration in this paper involve formation and breaking of covalent bonds. Prior experience has shown (provided the system remains electronically unexcited) that the structural chemistry involved can often adequately be represented by a linear combination of two-atom and three-atom component potentials.[4–6] In particular, this format is capable of conveying valency and bond directionality of the various elements involved.

In the present application only two atomic species appear, Si and F. The potential energy function Φ for a general two-species case A and B would have the following form:

$$\Phi=\sum v_{AA}+\sum v_{AB}+\sum v_{BB}+\sum v^{(3)}_{AAA}+\sum v^{(3)}_{AAB}+\sum v^{(3)}_{ABB}+\sum v^{(3)}_{BBB}. \tag{2.1}$$

Consequently, seven functions need to be specified, each of which must display translational and rotational invariance. Four of these [v_{AA},v_{BB},$v^{(3)}_{AAA}$, and $v^{(3)}_{BBB}$] normally would be available from modeling the pure elements A and B, respectively, requiring therefore only three more cross interactions.

We have previously developed combinations of two-atom and three-atom interactions to describe pure elemental silicon,[4] and pure elemental fluorine.[6] With the convention that A≡Si and B≡F, the respective pair interactions are

$$v_{AA}(r)=7.049\,556\,277(0.602\,224\,558\,4\,r^{-4}-1)\times\exp[(r-1.8)^{-1}]\quad(0<r<1.8)$$
$$=0\quad(1.8\leqslant r); \tag{2.2}$$

$$v_{BB}(r)=0.522\,76(0.112\,771\,r^{-8}-r^{-4})\times\exp\left[\frac{0.579\,495}{r-2.086\,182}\right]\quad(0<r<2.086\,182),$$
$$=0\quad(2.086\,182\leqslant r). \tag{2.3}$$

These expressions refer to a choice of units used throughout this paper: the length unit is $\sigma=0.209\,51$ nm, and the

 0021-9606/90/106239-07$03.00

energy unit is $\epsilon = 50.0$ kcal/mol $= 3.4723 \times 10^{-12}$ erg/atom. With this choice the silicon pair potential $v_{AA}(r)$ has a minimum of depth -1 at $r_e = 2^{1/6}$. Notice that v_{AA} and v_{BB} become identically zero beyond respective cutoffs, but that all their derivatives are continuous at those cutoffs. The latter attribute is especially significant for the stability and accuracy of molecular dynamics numerical algorithms.

Without any loss of generality, each three-atom interaction may be split into a sum of three parts, each a function of a pair of triangle side lengths and the included vertex angle

$$v^{(3)}_{XYZ}(\mathbf{r}_X,\mathbf{r}_Y,\mathbf{r}_Z) \equiv h_{XYZ}(r_{YX},r_{YZ},\theta_Y) + h_{YXZ}(r_{XY},r_{XZ},\theta_X) + h_{XZY}(r_{ZX},r_{ZY},\theta_Z). \quad (2.4)$$

The pure-element functions for Si and for F are

$$h_{AAA}(r,s,\theta) = 21 \exp\{1.2[(r-1.8)^{-1} + (s-1.8)^{-1}]\}(\cos\theta + \tfrac{1}{3})^2, \quad (2.5)$$

$$h_{BBB}(r,s,\theta) = 0.081\,818\,2(rs)^{-4} \exp\{0.579\,495[(r-2.086\,182)^{-1} + (s-2.086\,182)^{-1}]\} + (38.295 - 19.1475\cos^2\theta)\exp\{1.738\,485[(r-1.622\,586)^{-1} + (s-1.622\,586)^{-1}]\}, \quad (2.6)$$

where beyond the respective cutoffs (essential singularities) the terms are taken to be identically zero.

The cross interactions needed to complete the specification of our model are the following:

$$v_{AB}(r) = 21.234\,141\,38(0.569\,547\,643\,3\,r^{-3} - r^{-2}) \times \exp[1.3(r-1.8)^{-1}], \quad (2.7)$$

$$h_{BAB}(r,s,\theta) = [24(\cos\theta - \cos 103°)^2 - 3.2] \times \exp[(r-1.8)^{-1} + (s-1.8)^{-1}], \quad (2.8)$$

$$h_{ABB}(r,s,\theta) = 3.5 \exp[(r-1.8)^{-1} + (s-1.8)^{-1}], \quad (2.9)$$

$$h_{AAB}(r,s,\theta) = 15(\cos\theta + \tfrac{1}{3})^2 \exp[(r-1.8)^{-1} + (s-1.8)^{-1}], \quad (2.10)$$

$$h_{ABA}(r,s,\theta) = 50 \exp\{1.3[(r-1.8)^{-1} + (s-1.8)^{-1}]\}. \quad (2.11)$$

As before, each of these is to be taken as identically zero if a distance variable exceeds the essentially singular cutoff value. These cross interactions are the same as those used in our earlier study of silicon etching by high-density fluorine gas,[3] except that the multiplier in h_{ABB} has been increased from the earlier value 2.5 to the present value 3.5 shown in Eq. (2.9). This modification was implemented to weaken the one-end binding of F_2 molecules onto the crystalline silicon substrate, as discussed in Sec. IV.

The relative depths of the pair potentials v_{AA},v_{BB}, and v_{AB} are -1.000, -0.766, and -2.640. The respective bond lengths are 1.1225, 0.6849, and 0.7642.

The interactions defined by Eqs. (2.2)–(2.11) lead to reasonable structures for various gas-phase silicon fluorides. In particular SiF_2 is a bent triatomic with C_{2v} symmetry, SiF_3 is pyramidal with C_{3v} symmetry, and SiF_4 is tetrahedral (symmetry T_d). The last of these shows no tendency to bind a fifth fluorine atom covalently, thus exhibiting the silicon tetravalency. In a separate but related project[7] we have demonstrated that the SiF_4 and Si_2F_6 species form stable condensed phases at moderate temperatures in which the individual molecules retain their identities. Each of these properties accords with experimental observation, and thus lends credibility to our general model.

III. DYNAMICAL CONDITIONS

Our procedure requires generating a large number of trajectories for single F_2 molecules impinging on a crystalline Si substrate. Distinct classes of initial conditions have been used to assess the sensitivity of results to the initial F_2 translational and vibrational state.

A tetragonal unit cell with dimensions $14.656 \times 14.656 \times 50.000$, and periodic boundary conditions in all three directions, has been used for the dynamics. A 512-atom crystalline Si slab, consisting of 8 layers (3 with slight static buckling), stretches across the two short directions (x and y) of the unit cell. This slab is crystallographically oriented to expose (100) surfaces at top and bottom. The top surface has been reconstructed to form 32 dimers in a $p(2\times1)$ pattern. The 64 bottom surface atoms are rigidly held in bulk-crystal positions throughout our calculations, while the remaining 448 execute undamped, classical dynamical motions. Figure 1 illustrates the initial substrate geometry.

At the beginning of each trajectory the F_2 molecule was located above the slab. Its centroid was 2.2725 units in the z direction (normal to the slab surface) above the top layer of Si atoms, namely those forming surface dimers.

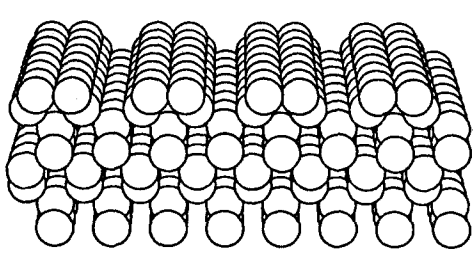

FIG. 1. Initial state of the unreacted silicon slab.

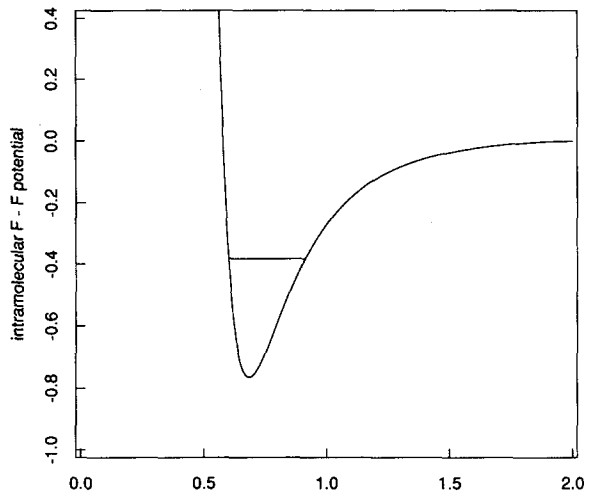

FIG. 2. Fluorine diatomic potential with the initial vibrational excitation level indicated for one class of initial trajectory conditions.

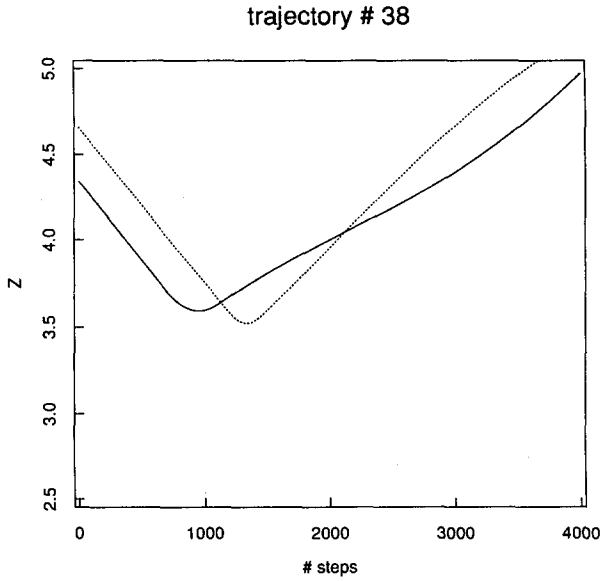

FIG. 3. Nonreactive trajectory, slow translation initial conditions. The two curves give the time dependence of fluorine atom z coordinates.

The horizontal position and the orientation of the diatomic were chosen randomly with uniform distributions. The initial height of the F_2 above the slab always assured that no fluorine–silicon interactions existed initially.

In order to keep interpretation of results as simple as possible, three classes of initial conditions have been invoked, for each one of which 105 trajectories have been numerically generated. They are as follows.

(1) *Slow translation.* The F_2 initially has no rotational or vibrational energy. The initial velocity of its centroid is directed downward toward the slab with speed

$$|v_z| = 0.2302 \tag{3.1}$$

the corresponding center of mass kinetic energy is equal to the mean center of mass kinetic energy of F_2 gas in equilibrium at temperature 603.7 K.

(2) *Rapid translation.* The initial conditions are the same as for the preceding case except that

$$|v_z| = 0.3988. \tag{3.2}$$

The equivalent temperature of equilibrated F_2 gas is 1811.0 K.

(3) *Vibrational excitation.* Initial conditions, including translational velocity (3.1) are the same as for "slow translation," except that F_2 is given a substantial vibrational excitation. This excitation is equal to half the dissociation energy of the diatomic, and is equivalent to a vibrational temperature of approximately 2×10^4 K. It is created simply by stretching the diatomic bond length to 0.9141. Figure 2 shows the fluorine diatomic bond potential and indicates the vibrational excitation level employed. It is obvious from the figure that vibrational dynamics at this level is quite anharmonic.

The silicon slab initially is at its own mechanically stable configuration, and its constituent atoms are at rest, for all cases considered.

The masses of the atoms are those of stable isotopic species

$$m_A(^{28}\mathrm{Si}) = 4.6457\times10^{-23}\ \mathrm{g},$$
$$m_B(^{19}\mathrm{F}) = 3.1548\times10^{-23}\ \mathrm{g}. \tag{3.3}$$

Classical equations of motion for the system of 450 movable atoms have been integrated using the fifth-order Gear predictor–corrector algorithm.[8] The natural time unit for the calculations is provided by the parameter combination

$$\tau = \sigma(m_A/\epsilon)^{1/2} = 7.6634\times10^{-14}\ \mathrm{s}. \tag{3.4}$$

The step length employed by our Gear algorithm was

$$\Delta t = 0.004\tau, \tag{3.5}$$

and each trajectory was followed for

$$4000\Delta t = 16\tau = 1.2261\ \mathrm{ps}. \tag{3.6}$$

In all cases this was enough elapsed time to permit surface collision to occur with subsequent dynamics sufficient to classify most aspects of the outcome.

IV. RESULTS

We have found that the dynamical trajectories can be classified according to four distinctive outcomes. Each of the three classes of initial conditions produces some of each of the four types, though the branching ratios quite clearly depend on the class of initial conditions involved.

Figures 3 through 6 illustrate the four outcomes with specific trajectories from the slow translation initial-condition class. These figures provide a time-dependent record of the z coordinates for the two fluorine atoms.

Figure 3 shows a typical nonreactive collision. The F_2 molecule simply bounces off the substrate into the vacuum

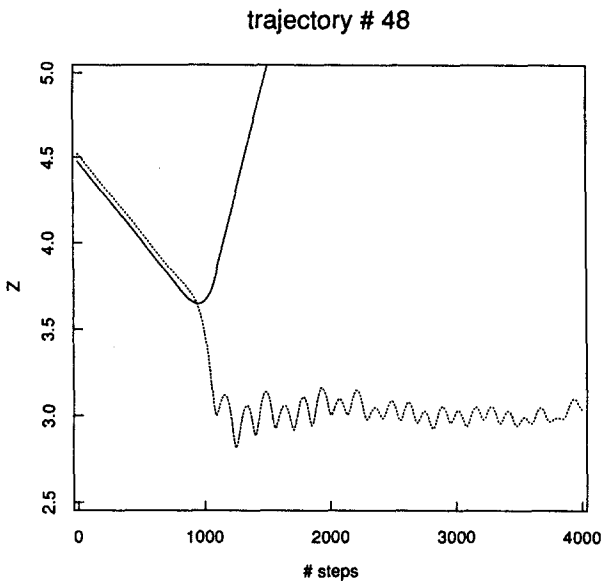

FIG. 4. Monofluorination trajectory, slow translation initial conditions.

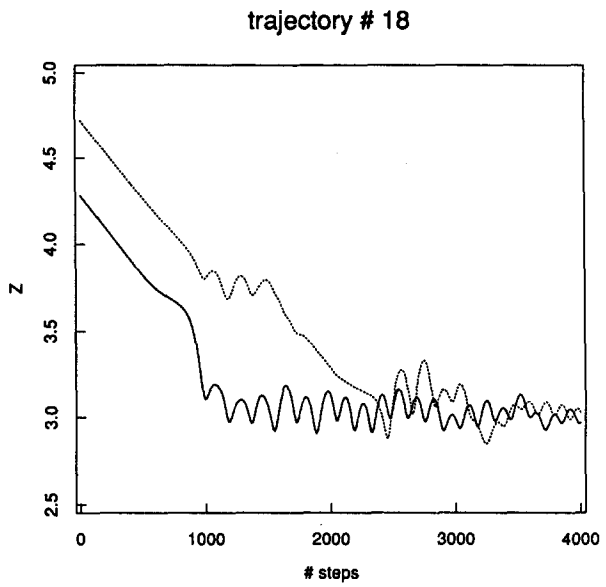

FIG. 5. Difluorination trajectory, slow translation initial conditions.

phase, picking up some slow rotational motion in the process. The vibrational degree of freedom, initially devoid of excitation in this slow translation case, remains virtually unexcited in the example shown. Likewise, very little energy is transferred to the rather rigid substrate.

Figure 4 shows a reactive encounter which leaves one fluorine atom bonded to the substrate, while the other fluorine is energetically expelled. The fluorination reaction is highly exothermic, and the energy released is partitioned between rapid translation of the emerging unbonded F atom, and vigorous vibration at the location of the bonded F atom. In all cases involving substrate fluorination, we find that it has been the dangling bonds at the initially three-coordinated surface dimer silicons that become occupied by fluorine atoms. The surface silicon dimers remain intact.

Figure 5 illustrates a surface collision that results in both atoms of the impinging F_2 becoming bonded to the substrate. Notice that in the specific example shown there appears to be a time lag of approximately 1500 Δt, or 0.46 ps, between formation of first and second Si–F covalent bonds.

The dynamical scenario presented in Fig. 6, as in the case of Fig. 4, involves monofluorination of the substrate. However the other F atom is not ejected but remains weakly bonded to the chemisorbed F. Evidently the excess energy of reaction from formation of the one covalent Si–F bond has been preferentially dumped into substrate vibrations. By following the dynamics for such trajectories much farther in time it is certainly possible that the physisorbed (weakly bound) F would eventually either evaporate from the surface, or vibrate toward a dangling bond on the surface and form a second Si–F covalent bond. Indeed, the trajectory exhibited in Fig. 5 could be interpreted as a quickly completed version of the latter of these alternatives. Figure 7 illustrates the reverse case, wherein a short-lived Si–F···F complex dissociates.

Potential energy minimizations have been carried out to clarify the nature of the weakly bound Si–F···F complex. First, the unreacted slab of 512 Si atoms, surface dimerized, has potential energy (in reduced units),

$$\Phi(\text{slab}) = -920.871\,00. \tag{4.1}$$

This results from the presence of 928 covalent Si–Si bonds, some of which are associated with the strained surface dimers. When a single F atom chemisorbs on the slab to occupy a dangling bond, the potential energy of the system changes to

$$\Phi(\text{F}) = -923.429\,38. \tag{4.2}$$

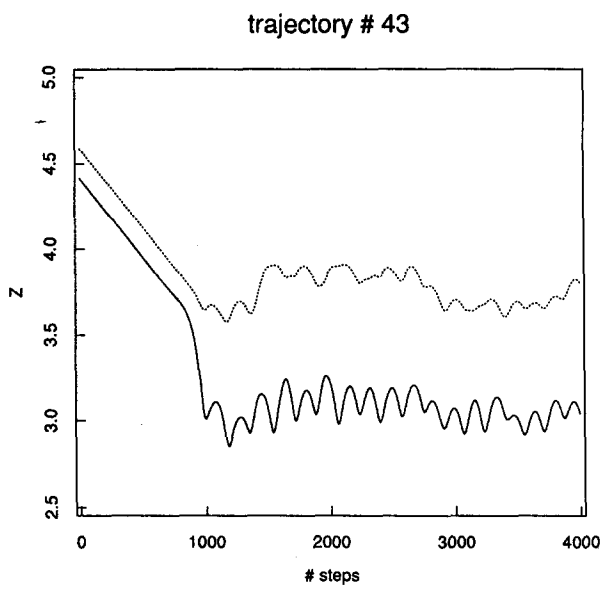

FIG. 6. Monofluorination with adsorption trapping of the other fluorine atom as a weakly bound Si–F···F complex.

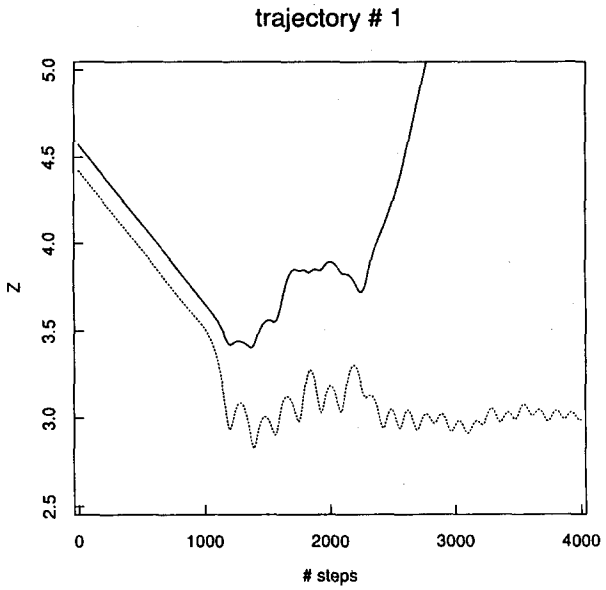

FIG. 7. Formation of a short-lined Si–F···F complex, followed by dissociation and ejection of the weakly bonded F atom.

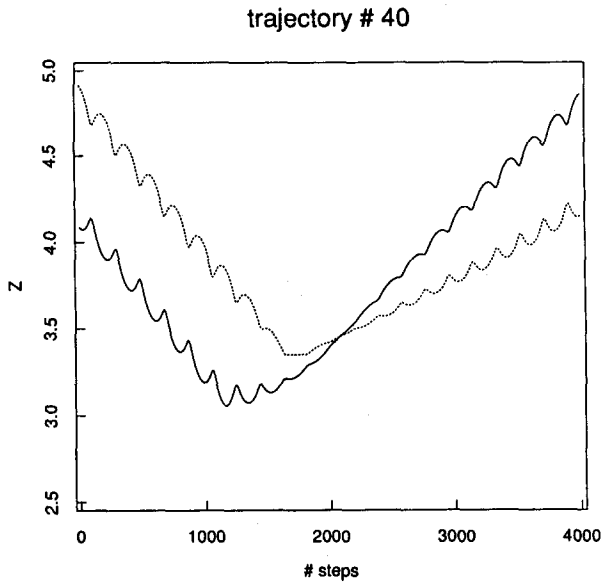

FIG. 8. Nonreactive trajectory with vibrational excitation initial conditions.

The shift, 2.558 38 units downward (127.92 kcal/mol), represents the chemisorption binding energy of a single free F atom. Finally, the addition of the second F atom to produce the weakly bound complex yields

$$\Phi(\mathrm{F}\cdots\mathrm{F}) = -923.468\,26. \tag{4.3}$$

This second downward shift is only 0.038 88 units (1.944 kcal/mol) and should be compared to the covalent bond strength of F_2 in the present model, namely 0.765 90 units (38.295 kcal/mol). Obviously this is far too weak to be classified as a covalent bond. This weak F···F bond at the potential minimum has length 0.7871 units (1.6492 Å), and points upward away from the surface. The equilibrium bond length for an isolated F_2 in the model is 0.6850 units (1.4351 Å).

Figure 8 presents a nonreactive trajectory from the "vibrational excitation" series. The scalloped shapes of the curves for both F atoms make it clear how anharmonic the vibrations are with the high degree of excitation used. Furthermore, the specific trajectory shown illustrates the behavior of all such cases, namely that little of the vibrational energy couples to the substrate during nonreactive collisions; the vibrational amplitudes for the incoming and outgoing diatomic molecules are roughly the same. In particular the vibrational excitation does not convert to extra translational kinetic energy of ejection from the surface.

Table I shows the numbers of trajectories of each of the four types (illustrated by Figs. 3 to 6), that emerged, respectively, from the three classes of initial conditions. The most obvious conclusion suggested by the entries is that increasing either initial translational or vibrational energy of the incident F_2 enhances its reactivity, since the proportion of unreactive trajectories declines for both such increases. This in turn suggests that most encounters between the diatomic molecule and the substrate involve a repulsive potential that must be surmounted in order for reaction to take place. Although the numbers involved are too small to have high statistical significance it seems, nevertheless, that increasing the initial vibrational energy is a more effective way of enhancing difluorination than is increasing initial translational energy, at least for those increments considered in this study. The formation and persistence of Si–F···F complexes over the observation period used (1.2261 ps) appears to have a probability that is rather insensitive to initial conditions, so that the minor fraction of trajectories experiencing this fate may not have had to surmount substantial potential energy barriers.

When difluorination occurs, the two fluorine atoms are always found chemisorbed close to one another. No substantial surface diffusion occurs between the two binding events. Three distinct difluorination patterns appear, each illustrated in Fig. 9. In the "opposing" pattern the fluorines occupy a pair of aligned dangling bonds, one from each of two surface dimers in neighboring rows whose covalent bonds are nominally coaxial. The "diagonal" pattern also utilizes a pair of dangling bonds from neighboring silicon dimer rows, but with misalignment by one dimer position. The "vicinal" pattern places the fluorines on the same side of neighboring silicon dimers in the same row.

Table II provides a breakdown of the difluorination

TABLE I. Numbers of trajectory types generated with the three classes of initial conditions.

	Slow translation	Rapid translation	Vibrational excitation
Nonreactive	45	17	24
Monofluorination	41	66	54
Difluorination	7	9	16
Si–F···F complex	12	13	11
Total	105	105	105

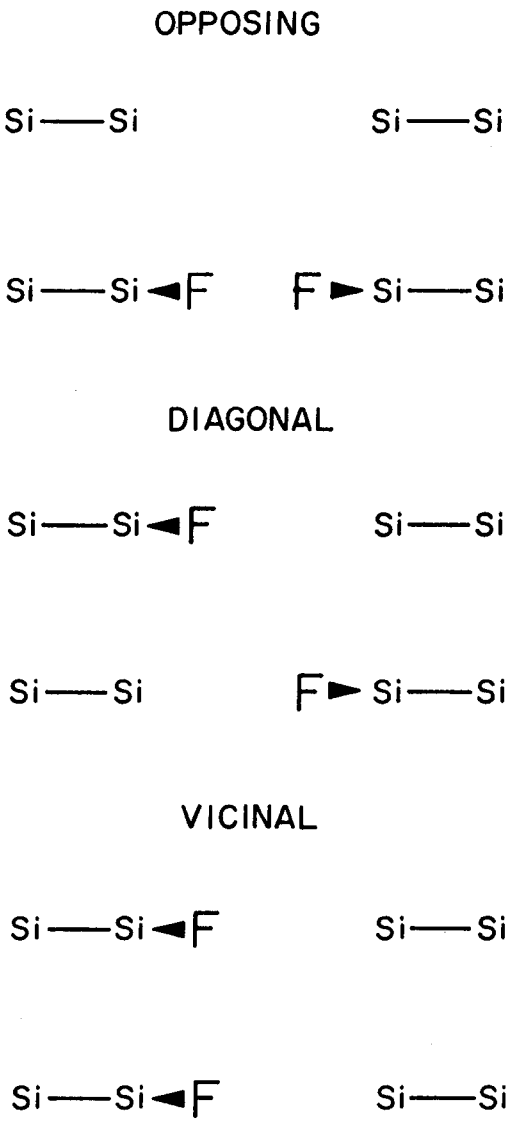

FIG. 9. Difluorination patterns observed on the dimerized top surface of the silicon slab.

trajectories, from each of the three classes of initial conditions, according to the final pattern observed. Once again only modest statistical significance can be claimed. Nonetheless it does appear that in the absence of substantial vibrational excitation the opposing pattern is the most likely outcome, followed by diagonal; the vicinal pattern is relatively infrequent. High vibrational excitation appears to disrupt this ordering, with diagonal and vicinal about equally likely as outcomes of difluorination, and opposing perceptibly less likely than either.

TABLE II. Relative occurrence probabilities for difluorination patterns for the three classes of initial conditions.

	Slow translation	Rapid translation	Vibrational excitation
Opposing	5	5	3
Diagonal	2	3	7
Vicinal	0	1	6
Total	7	9	16

V. DISCUSSION

This paper has been devoted to demonstrating feasibility for application of classical molecular dynamics simulation to study of surface chemical reactivity. The specific case examined involved collision of diatomic F_2 molecules with a dimerized, but otherwise unreacted, Si(100) surface. A linear combination of two-atom and three-atom interaction functions was used to represent the potential energy of arbitrary configurations of silicon and fluorine atoms. No claims are made herein that the interaction functions are an optimally accurate choice for the case under consideration, but the major features of the relevant structural chemistry are at least qualitatively reproduced. Given the large number of Si empirical potentials that have been proposed,[9–14] and an increasing body of quantum-mechanical information about silicon-fluorine interactions,[15–17] there is likely some fine tuning of interactions that could be implemented to improve upon the approximation we have used.

Doubtless other surface reactions could also be simulated with appropriate combinations of two-atom and three-atom interactions. Reactions of Cl_2 with Si or Ge substrates are interesting candidates for future study. Likewise, hydrogenation reactions would also be worth examining, though for most conditions quantum corrections to classical dynamics might have to be considered. Also (as pointed out before[3]) the reactant XeF_2, which is frequently used experimentally as a fluorine source for Si etching,[2,18] could also be represented by itself and in interaction with Si by a linear combination of two-atom and three-atom potentials.

Finally we stress that different selections of initial conditions for the F_2 + Si(100) surface reaction can be selected to fill out the dynamical picture for this system. Rotational excitation and nonnormal incidence would probably induce shifts in the dynamical branching, but have yet to be investigated. The same is true for initial elevated substrate temperature (it was at 0 K for the present study). In addition, different crystal surfaces could be compared for reactivity, including those with various defects. A very elaborate picture of reactive surface dynamics would emerge from such comprehensive simulation studies that could have great benefit for interpreting the results of STM chemisorption experiments.[19]

[1] G. A. Somorjai, *Chemistry in Two Dimensions: Surfaces* (Cornell University, Ithaca, 1981).
[2] F. R. McFeely, J. F. Morar, N. D. Shinn, G. Landgren, and F. J. Himpsel, Phys. Rev. B **30**, 764 (1984).
[3] F. H. Stillinger and T. A. Weber, Phys. Rev. Lett. **62**, 2144 (1989).
[4] F. H. Stillinger and T. A. Weber, Phys. Rev. B **31**, 5262 (1985).
[5] F. H. Stillinger and T. A. Weber, J. Phys. Chem. **91**, 4899 (1987).
[6] F. H. Stillinger and T. A. Weber, J. Chem. Phys. **88**, 5123 (1988).
[7] T. A. Weber and F. H. Stillinger (to be published).
[8] C. W. Gear, *Numerical Initial-Value Problems in Ordinary Differential Equations* (Prentice–Hall, Englewood Cliffs, 1971).
[9] R. Biswas and D. R. Hamann, Phys. Rev. B **36**, 6434 (1987).
[10] J. Tersoff, Phys. Rev. B **37**, 6991 (1988).

[11] M. I. Baskes, Phys. Rev. Lett. **59**, 2666 (1987).
[12] E. Kaxiras and K. C. Pandey, Phys. Rev. B **38**, 12736 (1988).
[13] D. W. Brenner and B. J. Garrison, Phys. Rev. B **34**, 1304 (1986).
[14] J. R. Chelikowsky, J. C. Phillips, M. Kamal, and M. Strauss, Phys. Rev. Lett. **62**, 292 (1989).
[15] B. J. Garrison and W. A. Goddard III, J. Chem. Phys. **87**, 1307 (1987).
[16] B. J. Garrison and W. A. Goddard III, Phys. Rev. B **36**, 9805 (1987).
[17] C. G. Van de Walle, F. R. McFeely, and S. T. Pantelides, Phys. Rev. Lett. **61**, 1867 (1988).
[18] H. F. Winters and J. W. Coburn, J. Vac. Sci. Technol. B **3**, 1376 (1985).
[19] R. Wolkow and P. Avouris, Phys. Rev. Lett. **60**, 1049 (1988).